

Improving Bond Strength of Translucent Zirconia Through Surface Treatment With $\text{SiO}_2\text{-ZrO}_2$ Coatings

Q Du • T Cui • G Niu • J Qui • B Yang

Clinical Relevance

The adhesion between coated zirconia and resin cement can be greatly improved using a layer of $\text{SiO}_2\text{-ZrO}_2$.

SUMMARY

Background: Translucent monolithic zirconia ceramics have been applied in dental clinics due to their esthetic translucent formulations and mechanical properties. Considering inherent ceramic brittleness, adhesive bonding with resin composite increases the fracture resistance of ceramic restorations. However, zirconia is a chemically stable material that is difficult to adhesively bond with resin.

†Qiao Du, DDS, Department of Stomatology, Beijing Integrated Traditional Chinese and Western Medicine Hospital, Beijing, China

†Tiehan Cui, DDS, Department of Oral and Maxillofacial Surgery, The First Affiliated Hospital of Nanchang University, Nanchang, China

*Guangliang Niu, DDS, Department of Stomatology, Beijing Integrated Traditional Chinese and Western Medicine Hospital, Beijing, China

*Jiaxuan Qui, DDS, Department of Oral and Maxillofacial Surgery, The First Affiliated Hospital of Nanchang University, Nanchang, China

Objectives: To investigate the influences of $\text{SiO}_2\text{-ZrO}_2$ coatings on adhesive bonding of zirconia and the surface characterization of those coatings.

Methods and Materials: Translucent zirconia discs were classified into groups based on surface treatments: CT (control), SB (sandblasting), C21 ($\text{SiO}_2\text{:ZrO}_2=2:1$), C11 ($\text{SiO}_2\text{:ZrO}_2=1:1$), and C12 ($\text{SiO}_2\text{:ZrO}_2=1:2$) ($n=10$). Surface characterization of coatings on zirconia were analyzed by scanning electron microscopy (SEM), energy-dispersive X-ray spectroscopy (EDX), surface roughness assessment (Ra), X-ray diffraction (XRD), water contact angle (WCA), translucency parameter (TP),

*Bin Yang, DDS, Restorative Department, College of Dentistry, University of Illinois at Chicago, IL, USA

†Tiehan Cui and Qiao Du contributed equally to this work.

*Corresponding authors: Dr Niu, No 3, East Street of Yongding Road, Beijing, 100039 China; e-mail: newgl@sina.com; Dr Qui, No 17, Yongwaizheng Street, Nanchang, 330006 China; e-mail: quijiaxuan@163.com; Dr Yang, 1200 West Harrison St, Chicago, 60612 IL, USA; e-mail: yangbin@uic.edu

<http://doi.org/10.2341/22-121-L>

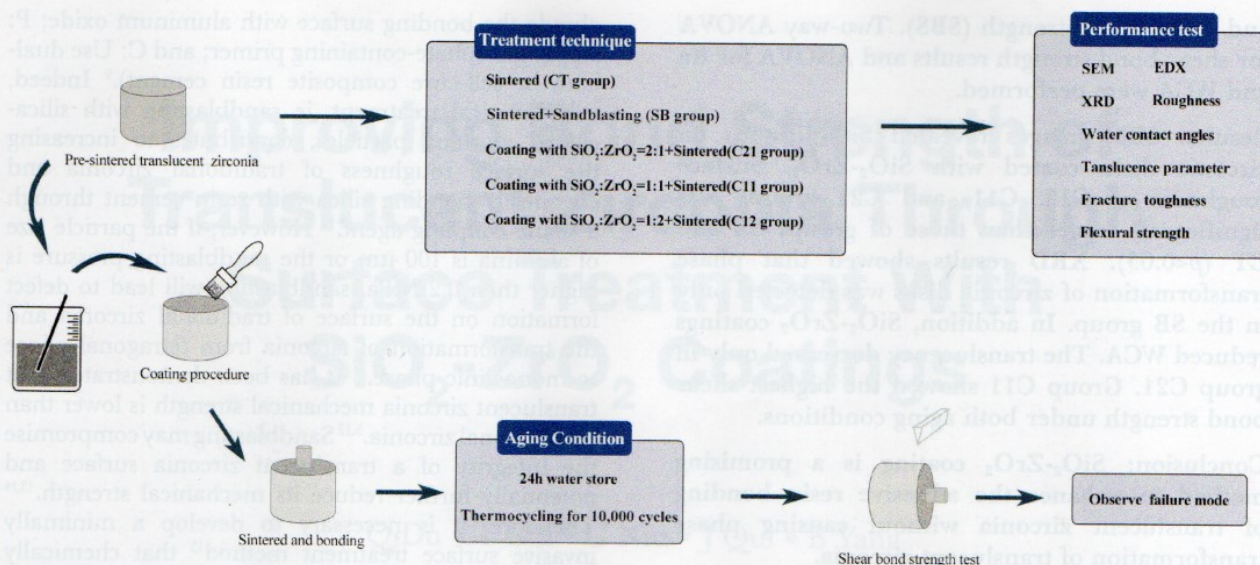


Figure 1. Experimental design.

under ultrasonication, three groups of $\text{SiO}_2\text{-ZrO}_2$ slurry were formulated based on the molar ratio of silica to zirconia: Si:Zr = 2:1, Si:Zr = 1:1, and Si:Zr = 1:2. The pH of the mixtures was set to 12 with the addition of 20% NaOH solution and the mixtures preserved in sealed glass bottles (Table 1).

Preparation of Specimens and Surface Treatments

Using a cutting machine (MICRACUT 176, Metkon, Turkey), the unsintered translucent zirconia blocks (3M ESPE Lava PLUS, Bad Säckingen, Germany) were sectioned into 100 discs with a diameter of 14 mm and a height of 5 mm. The discs were separated into five categories based on their surface treatment ($n=20$).

Group CT: The specimens were sintered according to the sintering protocol of the manufacturer. There was no surface treatment to specimens and CT served as the control group.

Group SB: The specimens were sintered according to the sintering protocol of the manufacturers, then sandblasted with 50 μm alumina particles for 10

seconds, perpendicularly applied onto the surface at a distance of 10 mm with a pressure of 0.2 MPa, followed by ultrasonic cleaning in ethanol for 5 minutes.

Group C21: The surface of pre-wetted zirconia specimens received a 0.02 mL slurry of Si:Zr = 2:1 with a small plastic brush producing a thin layer that was left to dry at room temperature (25°C). The zirconia specimens were then sintered according to the sintering protocol of the manufacturer (Table 2).

Group C11: The surface of pre-wetted zirconia specimens received a 0.02 mL slurry of Si:Zr = 1:1 with a small plastic brush producing a thin layer that was left to dry at room temperature (25°C). The zirconia specimens were then sintered according to the sintering protocol of the manufacturer (Table 2).

Group C12: The surface of pre-wetted zirconia specimens received a 0.02 mL slurry of Si:Zr = 1:2 with a small plastic brush producing a thin layer that was left to dry at room temperature (25°C). The zirconia specimens were then sintered according to the sintering protocol of the manufacturer (Table 2).

Table 1: Composition and Classification of $\text{SiO}_2\text{-ZrO}_2$ Coating Groups (by Mole Ratio of $\text{SiO}_2\text{:ZrO}_2$)

Coating Groups	Si/Zr	Silica Powder (g)	Zirconia Powder (g)	Polyethylene Glycol (g)	Water (mL)	pH
C21	2:1	0.3	0.308	1	10	12
C11	1:1	0.3	0.616	1	10	12
C12	1:2	0.15	0.616	1	10	12

Table 2: Cycle Parameters for Sintering Lava Plus

Cycle	Cycle Stages	Cycle Parameters
Standard sintering cycle	Drying	2 h in open, cold furnace or at room temperature
	Heating	20°C/min to 800°C
	Heating	10°C/min to 1450°C
	Holding time	120 min at 1450°C
	Cooling off	Maximum 15°C/min to 800°C
	Cooling off	Maximum 20°C/min to 250°C

SEM and EDX

Scanning electron microscopy (SEM, JSM-1900F, JEOL, Japan) was used to study the surface morphology of translucent zirconia subjected to various surface treatments at a voltage of 5.0 kV. Energy-dispersive X-ray spectroscopy was used to examine the elemental composition (EDX, AZtec X-Max 50, Oxford, UK). The elemental mapping approach was also used to examine the distribution of elements in the coatings.

Surface Roughness

An electromechanical profile meter (SJ-400 Mitutoyo, Yokohama, Japan) was used to assess the average surface roughness (Ra) of translucent zirconia following various surface treatments. To standardize roughness measurement, five distinct sites (one in the center and four in the borders) were chosen for each disc, and Ra values for each specimen were calculated as an average.

Water Contact Angle

The water contact angle (WCA) of zirconia surface was measured at 20°C using an OCA 50 automatic video optical contact angle measuring instrument (DAS-100, KRUS, Augustsburg, Germany). For the WCA test, 2 µL deionized water droplets were placed on the zirconia surface at a rate of 1.6 mL/minute through a micro-syringe, and the WCA value was determined within 1 minute.

X-Ray Diffraction Patterns

An X-Ray thin film diffractometer (D8 ADVANCE, Bruker, Karlsruhe, Germany) was used to study the wide-angle X-Ray diffraction (XRD) patterns of translucent zirconia surface treated with monochromatic Cu K radiation following various surface treatments. The spectra were collected in two-angle ranges of 10-65° in increments of 0.02° and in step sizes of 1 second. 40 kV and 40 mA were chosen as the operating voltage and current, respectively.

Translucence Parameter

One dental colorimeter (ShadeEye NCC, Shofu, Japan) was used to measure color parameters (L^* , lightness; a^* , redness-greenness; b^* , yellowness-blueness) of each specimen under black (B) and white (W) backgrounds three times, and then the three readings were averaged. The colorimeter probe was perpendicular to the surface of each specimen, and the dental colorimeter was recalibrated after every five readings. We calculated the translucence parameter (TP) using $TP = \sqrt{(L_B^* - L_W^*)^2 + (a_B^* - a_W^*)^2 + (b_B^* - b_W^*)^2}$.

Preparation of Bond Strength Specimens

Each group of specimens was etched with hydrofluoric acid gel for 90 seconds, then washed with water spray for 30 seconds, and finally air-dried. A 0.07 mm thick paper sticker with a center hole (diameter 3 mm) was affixed to the surface of the specimen to limit the bonding area (ISO/TS 11405 Dentistry—Testing of adhesion to tooth structure).²⁰ This restricts surface treatment of the substrate, allows demarcation of the extent of the adhesive, and allows accurate measurement of bonded surface.

Prior to cementation, a primer containing phosphate ester monomer and silane coupling agent (Single Bond Universal, 3M ESPE) was applied to the bonding surface of the translucent zirconia disks for 20 seconds. Subsequently, direct gentle air was blown on the specimen surface for approximately 5 seconds until the solvent in the silane coupling agent evaporated completely.

Cylinders with a diameter of 3.5 mm and a height of 4 mm were manufactured using composite resin (Filtek Bulk Fill, 3M ESPE) and stored in water for seven days. Before bonding, one side of the resin cylinders was polished with 600 mesh SiC sandpaper, then cleaned with ultrasonic water for 5 minutes, and finally dried. The resin cement (RelyX Ultimate, 3M ESPE) was activated according to the manufacturer's instructions and applied to the treated zirconia surface. The composite resin cylinders were cemented

to the bonding area under a pressure of 20 N. After the removal of excess cement, all the specimens were light-cured for 20 seconds on each side using the 800 mW/cm² light-curing device (Elipar 2500, 3M ESPE) with a distance of 2 cm. The specimens were then placed in a box with relative humidity of 100% and room temperature of 25°C for 1 hour. In this study, five groups (n=20) were created, each of which was divided into two subgroups and subjected to two aging conditions: water storage at 37°C for 24 hours (n=10) or with additional 10,000 thermal cycles of 5.0 ± 0.5°C to 55.0 ± 0.5°C with a 30-second dwell duration (Prototech, New York, NY, USA) (n=10), prior to shear bond strength testing.

Shear Bond Strength

The shear bond strength (SBS) test was performed. All specimens were fixed and measured using a universal testing machine (3367 Instron, Norwood, MA, USA). A continuous load of 500 N was applied at a crosshead speed of 1.0 mm/minute. The SBS was calculated by dividing the load force at fracture (N) by the area of bonded ceramic (mm²).

Failure Mode Evaluation

All fracture specimens collected from the SBS test were inspected using an optical microscope (SmartScope MVP 200, Portland, USA) at a magnification of 6.5×. Fracture modes were defined as: 1) "Adhesive failure" at the interface between resin cement and translucent zirconia; 2) "Cohesive failure" within resin cement; and 3) "Mixed failure" as a combination of adhesive failure and cohesive failure.

Statistical Analysis

Using the Statistical Package for Social Sciences (SPSS version 20.0), two-way analysis of variance (ANOVA) for shear bond strength results and one-way ANOVA for other data was performed at a significance level of $\alpha=0.05$.

RESULTS

Surface Roughness, Surface Morphology, and Chemical Composition

The measured Ra of translucent zirconia specimens is listed in Table 3. The Ra in group C21 (2.17±0.58 μm) was significantly higher than that in other groups ($p<0.05$). In addition, the Ra of group SB (0.46±0.03 μm) was significantly lower than those of SiO₂-ZrO₂-coated specimens in group C11 (1.46±0.21 μm), in group C12 (1.33±0.10 μm), and in group C21 (2.17±0.58 μm) ($p<0.05$). The Ra of group C11 (1.46±0.21 μm) did not differ significantly from that of group C12 (1.33±0.10 μm) ($p>0.05$).

SEM images of the coating surface in various treated translucent zirconia specimens are shown in Figures 2 and 3. In the control group, compared with the other groups, the surface of as-sintered zirconia appeared to be the smoothest. Compared with the control group, the surface of translucent zirconia treated by sandblasting was irregular and rougher. For groups coated with SiO₂-ZrO₂, ie, groups C21, C11, and C12, many "SiO₂ islands" were observed on the surface of translucent zirconia (Figure 3B, E, H-yellow circles). In fact, many valleys appeared to be SiO₂ islands (Figure 3B, E-blue squares). Moreover, many zirconium atoms (Figure 2C, F, I-red arrows) were embedded in SiO₂ islands in groups C21 and C11. However, the valleys of group C12 were shallower than those of other groups, rendering a honeycomb structure.

The elemental composition of the translucent zirconia surfaces after various treatments were indicated in EDX results (Figure 4). The silicon content on the surface of translucent zirconia in group C21 was the highest. In comparison, the silicon content on the surface of translucent zirconia in C11 and C12 groups gradually decreased.

The element spatial distributions of Si and O on the coated surface of translucent zirconia specimens are shown in EDX mapping (Figure 5). The silica

Table 3: Surface Characterization of All the Test Groups (n = 10)^a

Group	CT	SB	C21	C11	C12
Ra	0.26±0.054 a	0.46±0.027 b	2.17±0.575 c	1.46±0.211 d	1.33±0.103 d
WCA	84.70±0.408 a	63.90±2.092 b	65.80±3.827 b	58.12±1.635 c	63.23±0.991 b
TP	12.13±0.666 a	12.03±0.513 a	8.67±0.808 b	12.20±0.265 a	11.93±0.306 a

Abbreviations: CT, sintered; C21, C11, and C12: SiO₂/ZrO₂ = 2:1, 1:1 and 1:2; Ra, roughness assessment; SB, sandblasting; TP, translucence parameter; WCA, water contact angles.

^aDifferent lowercase letters indicate significant differences ($p<0.05$).

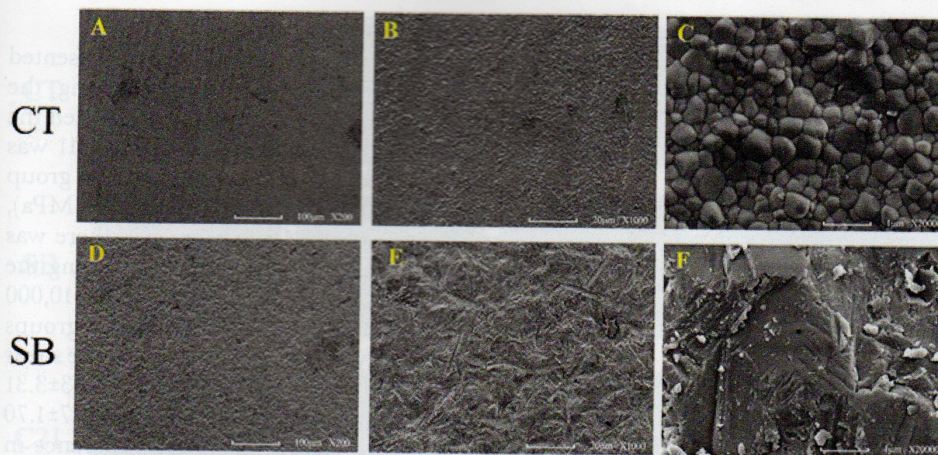


Figure 2. SEM images of the surface of the translucent zirconia with sintered (CT group) and sandblasting (SB group) at a magnification of 200 \times , 1000 \times , and 20,000 \times . In the CT group, the surface of translucent zirconia appeared to be smooth. In the SB group, the surface of translucent zirconia was irregular and rougher.

particles were uniformly distributed on the SiO₂-ZrO₂-coated surface of translucent zirconia in group C12. Nevertheless, in the C21 group, the silica particles on the SiO₂-ZrO₂-coated surface of translucent zirconia aggregated into a pile. Furthermore, the distribution of the silica particles on the SiO₂-ZrO₂-coated surface of translucent zirconia in group C11 was not as uniform as that in group C21.

Water Contact Angle

The results of WCA are shown in Table 3. WCA differed dramatically in specimens with different surface

treatments. The WCA was reduced in both group SB and the groups with coating. In group C11, the WCA was determined to be the lowest in all groups ($p < 0.05$).

Phase Transformation

The XRD diffraction patterns with various surface treatments are shown in Figure 6. Tetragonal (T) phase and cubic (C) phase structures could be detected on the surface of any translucent zirconia surface. The peak value of monoclinic phase appeared at a 2 θ angle of 28.47 $^\circ$ (arrow shown in Figure 6), which was detected only on the surface in group SB.

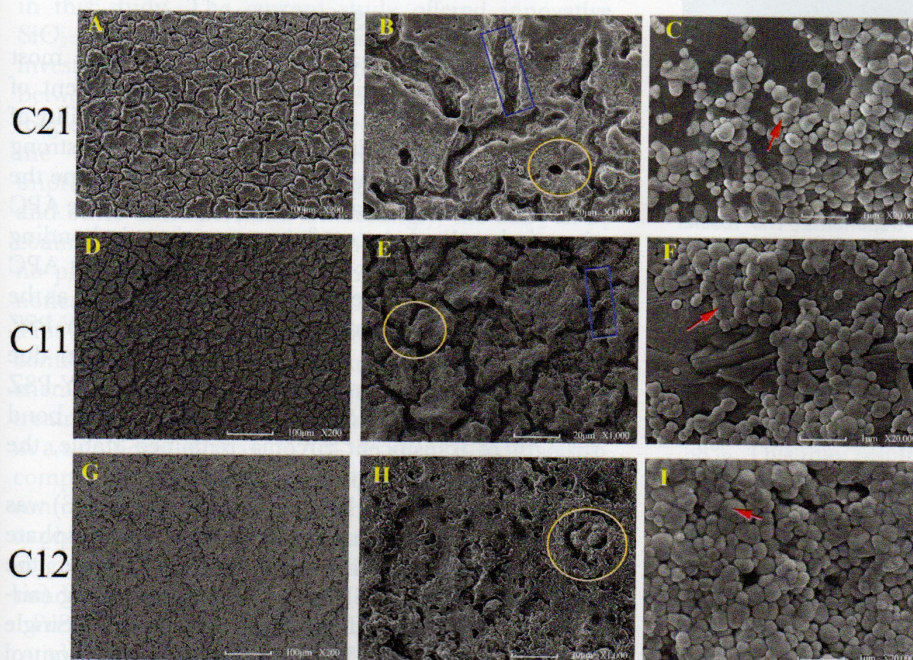


Figure 3. SEM images of the surface of the coated translucent zirconia for C21 group, C11 group and C12 group at a magnification of 200 \times , 1000 \times , and 20,000 \times . In C21, C11, and C12 groups, many "SiO₂ islands" were observed on the surface of translucent zirconia (B, E, H-yellow circles); many zirconium atoms were embedded in SiO₂ islands of C21 and C11 groups (C, F, I-red arrows). However, the valleys of group C12 were shallower than those of other groups, rendering a honeycomb structure (B, D-blue squares).

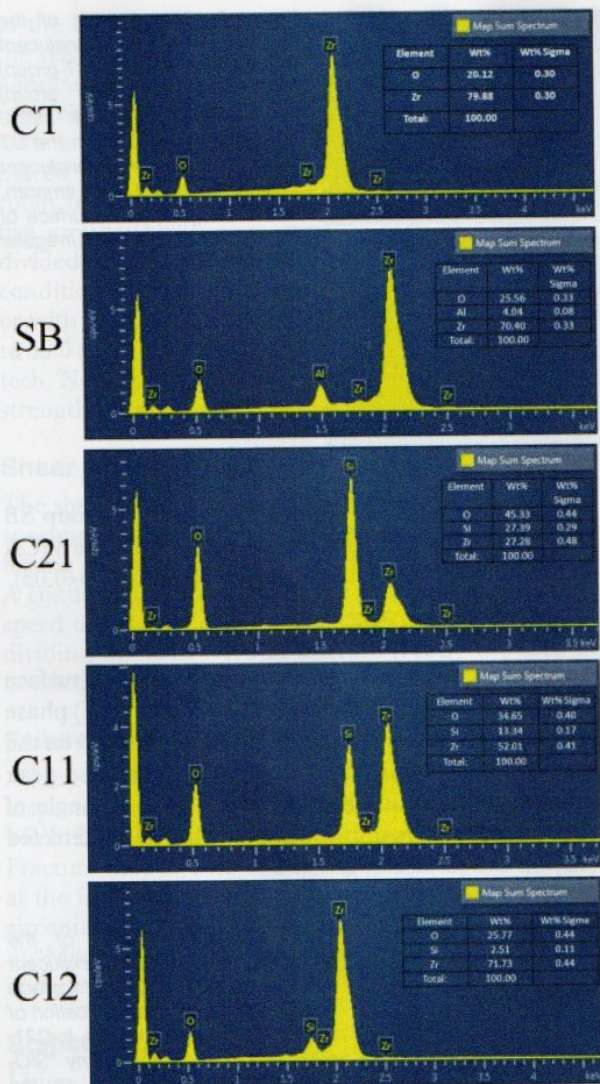


Figure 4. EDX patterns and elemental composition of translucent zirconia specimens after the various treatments. The results showed the distribution of elements in all groups and the mass fraction of each element. Abbreviations; CT: sintered, C21, C11 and C12: $\text{SiO}_2/\text{ZrO}_2 = 2:1, 1:1$ and $1:2$; SB: sandblasting.

Translucence Parameters

It was found that sandblasting did not reduce the translucency parameters of translucent zirconia (see Table 3). For the $\text{SiO}_2\text{-ZrO}_2$ coating treatment, the translucency parameters of the C21 group with a higher silicon atom ratio were significantly lower ($p < 0.05$) than those of other groups, while no significant difference was found among groups C11, C12, and control.

Shear Bond Strength

The results of the shear bond strength test are presented in Table 4. Under the condition of 24-hour aging, the shear bond strength of the control group exhibited the lowest (10.91 ± 1.31 MPa), while that of group C11 was the highest (25.11 ± 2.30 MPa) value followed by group C21 (20.8 ± 2.30 MPa), group C12 (19.00 ± 2.04 MPa), and group SB (14.67 ± 2.10 MPa). Moreover, there was a statistically significant difference ($p < 0.05$) among the five groups (Table 4). Under the condition of 10,000 thermal cycles, the shear bond strength of all groups decreased significantly ($p < 0.05$). Furthermore, the shear bond strength of group C11 was the highest (12.53 ± 3.31 MPa) while that of group CT was lowest (3.77 ± 1.70 MPa). However, there was no significant difference in shear bond strength between the C21 group and the C12 group ($p > 0.05$).

Failure Mode Analysis

Failure mode analysis of the debonding specimens after the shear bond strength test showed that the failure mode of each specimen was mainly mixed failure (Table 5). After 10,000 thermal cycles of artificial aging, the adhesion between resin cement and translucent zirconia surface in all groups decreased. The percentage of adhesive failure was higher in the control group, while the percentage of mixed failure was higher in group SB, and cohesive failure occurred only in groups with coating.

DISCUSSION

Monolithic zirconia has emerged as one of the most popular dental materials due to the development of digital dentistry.²¹ This is due to the chemical stability of zirconia, which makes it challenging to establish a strong and durable bonding with the resin.²² To overcome the adhesion challenge, Blatz and others proposed the APC zirconia bonding concept.⁹ A strong zirconia bonding can be established for 3Y-TZP by applying the APC zirconia-bonding concept.²³ In one previous study, as the crystalline phase in translucent zirconia such as 4Y-PSZ and 5Y-PSZ changed with phase transformation due to sandblasting, the mechanical strength of 4Y-PSZ and 5Y-PSZ decreased.²⁴ While the short-term bond strength of translucent zirconia remained stable, the long-term bond strength remains unknown.

In this study, Single Bond Universal (3M ESPE) was used as a chemical ceramic primer containing phosphate ester monomer (APC-P) and silane. Therefore, the specimens in group SB underwent sandblasting (air-abrasion: APC-A) and chemical application of Single Bond Universal (APC-P), serving as the positive control

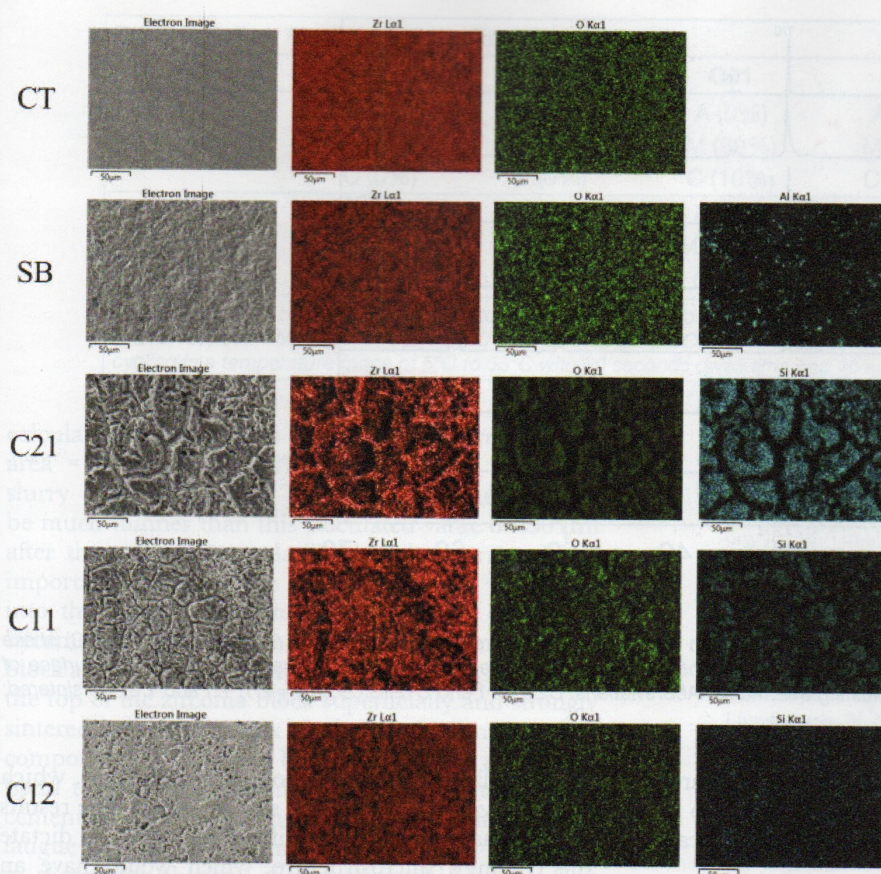


Figure 5. EDX mapping of the spatial distribution of elements Zr, Si, and O in the $\text{ZrO}_2\text{-SiO}_2$ coatings. Zr and O elements were detected in any groups. Al was detected by sandblasting group and Si was detected in $\text{SiO}_2\text{-ZrO}_2$ coating groups. Abbreviations: C21, C11 and C12: $\text{SiO}_2/\text{ZrO}_2 = 2:1, 1:1$ and $1:2$; CT, sintered, SB: sandblasting.

in this study. The current study offered innovative $\text{SiO}_2\text{-ZrO}_2$ coatings applied to translucent zirconia and investigated their influence on the shear bond strength between resin and the translucent zirconia, comparing to groups SB and CT. Compared with the CT group, the $\text{SiO}_2\text{-ZrO}_2$ coatings demonstrated significant improvement in terms of roughness, surface energy, and other characteristics. Interestingly, the $\text{SiO}_2\text{-ZrO}_2$ coating did not affect transmittance (Table 3) and no phase transformation on the zirconia surface was noticed as demonstrated in the XRD results (Figure 6). This finding is in agreement with other studies^{25,26} and contributes to a treated zirconia surface for durable chemical bonding. In this study, zirconia surface treatment with $\text{SiO}_2\text{-ZrO}_2$ coating (group C11) resulted in a significant increase (>70%) in shear bond strength compared with sandblasting treatment (group SB). In contrast, our results indicated that the sandblasting led to phase transformation on translucent zirconia surface in group SB (Figure 6), which possibly reduced the bonding strength.

Previous studies indicated that increased surface roughness, sandblasting, and tribochemical silica

coating techniques can strengthen the bonding between zirconia and resin.^{25,27} Tribochemical silica coating is more effective than sandblasting because the silica introduced to the bonding substrate surface can form chemical bonding bonds.¹ The chemical bonding can be achieved using silica, which forms strong siloxane (Si-O-Si) connections by condensation with silane.²⁸ The $\text{SiO}_2\text{-ZrO}_2$ coating technique in this research improves durable bonding through a similar mechanism as tribochemical silica coating to form chemical bonding between SiO_2 and resin. In this study, the SBS decreased in all groups after artificial thermal cycling (Table 4). However, the shear bond strength of groups CT and SB were reduced by 65% and 52%, respectively, while shear bond strength was reduced in groups using coating by 38%. This may result from the $\text{SiO}_2\text{-ZrO}_2$ coating silica component being primarily responsible for creating a strong bond with the resin (Figure 2). Additionally, compared to group SB, translucent zirconia had better wettability in the $\text{SiO}_2\text{-ZrO}_2$ coating group (Table 3). The high percentage of cohesive fracture modes in coating groups further suggested that $\text{SiO}_2\text{-ZrO}_2$ coating created a strong and durable bonding (Table 5),

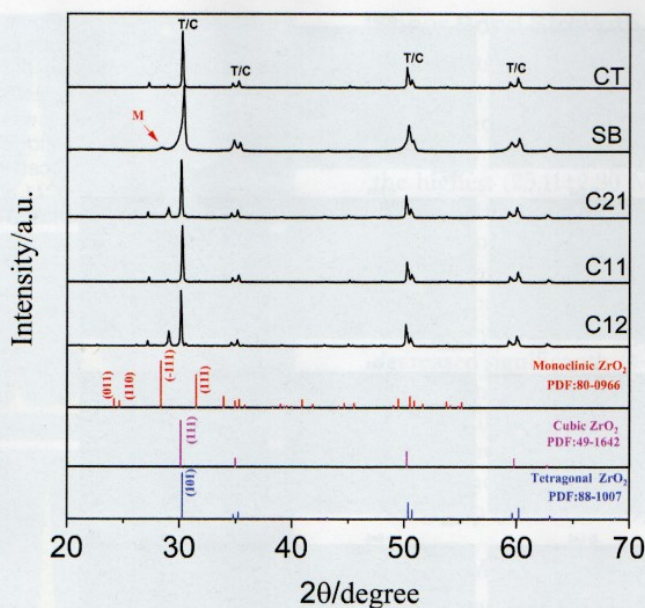


Figure 6. XRD patterns of translucent zirconia specimens with the various surface treatments: Tetragonal (T) phase and cubic (C) phase structure could be detected on the surface of any translucent zirconia surface. The monoclinic phase was detected on the surface of translucent zirconia specimens with sandblasting treatments. Abbreviations: C21, C11 and C12: $\text{SiO}_2/\text{ZrO}_2 = 2:1, 1:1$ and $1:2$; CT: sintered; SB, sandblasting.

while there was a higher percentage of adhesive failure in group SB, indicating that sandblasting did lead to a stable durable resin bonding through micro-mechanical retention (Table 5).

For groups coating with the different $\text{SiO}_2\text{-ZrO}_2$ ratios used in this study, the shear bond strength varied significantly (Table 4). As shown in Figure 3, the coatings with different $\text{SiO}_2\text{-ZrO}_2$ ratios created a rougher surface and increased the bonding through mechanical interlocking. Moreover, as shown in EDX results and the wettability test, the coating treatment increased the silicon content on the translucent zirconia surface, which in turn increased the surface energy after coating.²⁹ Other coating methods could be compared with $\text{SiO}_2\text{-ZrO}_2$ coating treatment. According to a previous study, Lung and others coated the SiO_2 coating on zirconia via decomposing silicon nitride hydrolysis.³⁰ This method may be better

than sandblasting in terms of aging resistance, which changes with the number of silicon atoms. The results showed that the number of silicon atoms would dictate the coating's microstructure, which would have an impact on the bond strength.

In this study, very thin layers of $\text{SiO}_2\text{-ZrO}_2$ were coated on translucent zirconia via sintering to improve resin bonding by increasing SiO_2 content on the zirconia surface and promoting chemical bonding, and by increasing surface roughness and surface area. One limitation of this study is that the thickness of the coatings was not measured due to some restrictions. However, to make the thickness of each specimen's surface consistent and under control, each specimen surface was coated with 0.02 mL ceramic slurry and the thickness of the 130 μm slurry was calculated. According to the amount of powder added, powder density and distilled water, the coating thickness was

Table 4: Shear Bond Strength (MPa) of All the Test Groups ($n = 10$)^a

Test Group	CT	SB	C21	C11	C12
24h	10.91±1.31 Aa	14.67±2.10 Ba	20.80±2.30 Ca	25.11±2.69 Da	19.00±2.04 Ea
TC10,000	3.77±1.70 Ab	6.94±2.30 Bb	12.53±3.31 Cb	16.38±2.55 Db	11.76±2.37 Cb

Abbreviations: C21, C11, and C12, $\text{SiO}_2/\text{ZrO}_2 = 2:1, 1:1$ and $1:2$; CT, sintered; TC, thermal cycling in a temperature range of 5°C to 55°C with 30 s dwell time and 10 s transfer time; SB, sandblasting; 24 h, 24 hours of water storage.

^aDifferent lowercase letters in the same column and different uppercase letters in the same row indicate significant differences ($p < 0.05$).

Test Group	CT	SB	C21	C11	C12
Group 24 h	A (40%)	A (10%)	A (0%)	A (0%)	A (0%)
	M (60%)	M (90%)	M (90%)	M (80%)	M (100%)
	C (0%)	C (0%)	C (10%)	C (20%)	C (0%)
Group TC	A (80%)	A (40%)	A (0%)	A (0%)	A (0%)
	M (20%)	M (60%)	M (100%)	M (90%)	M (100%)
	C (0%)	C (0%)	C (0%)	C (10%)	C (0%)

Abbreviations: 24 h, 24 hours of water storage; A, M, and C represent adhesive failure, mixed failure, and cohesive failure, respectively; CT, sintered; C21, C11, and C12, SiO₂/ZrO₂ = 2:1, 1:1 and 1:2; SB, sandblasting; TC, thermal cycling in a temperature range of 5°C to 55°C with 30 seconds dwell time and 10 seconds transfer time.

calculated as: Thickness = Volume of slurry/Surface area = 0.02 mL/π(14/2)² mm² ≈ 130 μm, when the slurry coating was wet. The actual thickness should be much thinner than this calculated value of 130 μm after the solvent was volatilized and sintering. More importantly, part of the SiO₂-ZrO₂ slurry infiltrated into the pores of the underlying zirconia block and became sintered together with the underlying zirconia block after sintering. Therefore, the coatings formed on the top of the zirconia block superficially and strongly sintered into the zirconia block. In addition, the glass component (SiO₂) would be helpful to form a chemical bond to the resin cement through silanization at the cementation step of zirconia restorations. Under fatigue cycling, cracks may generate and propagate in the glassy phase of the coating, which may affect the mechanical strength of the system. Therefore, the influence of coating thickness on the mechanical properties will be investigated in the future.

CONCLUSIONS

Within the limits of this study, the following conclusions can be drawn: SiO₂-ZrO₂ coating is a promising method to enhance the adhesive resin bonding of translucent zirconia without causing phase transformation of translucent zirconia.

Conflict of Interest

The authors of this article certify that they have no proprietary, financial, or other personal interest of any nature or kind in any product, service, and/or company that is presented in this article.

(Accepted 13 March 2023)

REFERENCES

- Zhang Y & Lawn BR (2018) Novel zirconia materials in dentistry *Journal of Dental Research* 97(2) 140-147. <https://doi.org/10.1177/0022034517737483>
- Thammajaruk P, Inokoshi M, Chong S, & Guazzato M (2018) Bonding of composite cements to zirconia: A systematic review and meta-analysis of *in vitro* studies *Journal of the Mechanical Behavior of Biomedical Materials* 80 258-268. <https://doi.org/10.1016/j.jmbbm.2018.02.008>
- Stawarczyk B, Keul C, Eichberger M, Figge D, Edelhoff D, & Lümkmann N (2017) Three generations of zirconia: From veneered to monolithic. Part II *Quintessence International* 48(6) 441-450. <https://doi.org/10.3290/j.qi.a38157>
- Stawarczyk B, Keul C, Eichberger M, Figge D, Edelhoff D, & Lümkmann N (2017) Three generations of zirconia: From veneered to monolithic. Part I *Quintessence International* 48(5) 369-380. <https://doi.org/10.3290/j.qi.a38057>
- Zhang Y (2014) Making yttria-stabilized tetragonal zirconia translucent *Dental Materials* 30(10) 1195-1203. <https://doi.org/10.1016/j.dental.2014.08.375>
- Harianawala HH, Kheur MG, Apte SK, Kale BB, Sethi TS, & Kheur SM (2014) Comparative analysis of transmittance-for different types of commercially available zirconia and lithium disilicate materials *Journal of Advanced Prosthodontics* 6(6) 456. <https://doi.org/10.4047/jap.2014.6.6.456>
- Ruales-Carrera E, Cesar PF, Henriques B, Fredel MC, Özcan M, & Volpato CAM (2019) Adhesion behavior of conventional and high-translucent zirconia: Effect of surface conditioning methods and aging using an experimental methodology *Journal of Esthetic and Restorative Dentistry* 31(4) 388-397. <https://doi.org/10.1111/jerd.12490>
- Franco-Tabares S, Stenport VF, Hjalmarsson L, Tam PL, & Johansson CB (2019) Chemical bonding to novel translucent zirconias: A mechanical and molecular investigation *Journal of Adhesive Dentistry* 21(2) 107-116. <https://doi.org/10.3290/j.jad.a42361>
- Blatz MB, Alvarez M, Sawyer K, & Brindis M (2016) How to bond zirconia: The APC concept 37(9) 611-617. <https://pubmed.ncbi.nlm.nih.gov/27700128>
- Chen B, Yan Y, Xie H, Meng H, Zhang H, & Chen C (2020) Effects of tribochemical silica coating and alumina-particle air abrasion on 3Y-TZP and 5Y-TZP: Evaluation of surface hardness, roughness, bonding, and phase transformation *Journal of Adhesive Dentistry* 22(4) 373-382. doi: 10.3290/j.jad.a44868
- Zhao P, Yu P, Xiong Y, Yue L, Arola D, & Gao S (2020) Does

- the bond strength of highly translucent zirconia show a different dependence on the airborne-particle abrasion parameters in comparison to conventional zirconia? *Journal of Prosthodontic Research* **64**(1) 60-70. <https://doi.org/10.1016/j.jpor.2019.04.008>
12. Alammar A & Blatz MB (2022) The resin bond to high-translucent zirconia—A systematic review *Journal of Esthetic and Restorative Dentistry* **34**(1) 117-135. <https://doi.org/10.1111/jerd.12876>
 13. Shimizu H, Inokoshi M, Takagaki T, Uo M, & Minakuchi S (2018) Bonding efficacy of 4-META/MMA-TBB resin to surface-treated highly translucent dental zirconia *Journal of Adhesive Dentistry* **20**(5) 453-459. <https://doi.org/10.3290/j.jad.a41330>
 14. Okada M, Taketa H, Torii Y, Irie M, & Matsumoto T (2019) Optimal sandblasting conditions for conventional-type yttria-stabilized tetragonal zirconia polycrystals *Dental Materials* **35**(1) 169-175. <https://doi.org/10.1016/j.dental.2018.11.009>
 15. Akar GC, Pekkan G, Çal E, Eskitaşçıoğlu G, & Özcan M (2014) Effects of surface-finishing protocols on the roughness, color change, and translucency of different ceramic systems *Journal of Prosthetic Dentistry* **112**(2) 314-321. <https://doi.org/10.1016/j.prosdent.2013.09.033>
 16. Akay C, Okşayan R, & Özdemir H (2020) Influence of various types of surface modifications on the shear bond strength of orthodontic brackets on Y-TZP zirconia ceramics *Journal of the Australian Ceramics Society* **56** 1435-1439. <https://doi.org/10.1007/s41779-020-00479-9>
 17. Zhou H, Yu C, Qi C, Qiu D, Zhang S, Li J, & Hu Y (2020) Effect of femtosecond laser and silica coating on the bond strength of zirconia ceramic *Advances in Applied Ceramics* **119**(5-6) 276-283. <https://doi.org/10.1080/17436753.2020.1780552>
 18. Çakırbay Taniş M, Akay C, & Şen M (2019) Effect of selective infiltration etching on the bond strength between zirconia and resin luting agents *Journal of Esthetic and Restorative Dentistry* **31**(3) 257-262. <https://doi.org/10.1111/jerd.12441>
 19. Du Q & Niu G, Lin H, & Jiang R (2015) Effect of SiO₂-ZrO₂ slurry coating on surface performance of zirconia ceramic *Chinese Journal of Stomatology* **50**(11) 681-684. <https://pubmed.ncbi.nlm.nih.gov/26757764/>
 20. ISO/TS 11405 Dentistry—Testing of adhesion to tooth structure, *Geneve: International Organization for Standardization* 2015.
 21. Alqutaibi AY, Ghulam O, Krsoum M, Binmahmoud S, Taher H, Elmalky W, & Zafar MS (2022) Revolution of current dental zirconia: A comprehensive review *Molecules* **27**(5) 1699. <https://doi.org/10.3390/molecules27051699>
 22. Bapat RA, Yang HJ, Chaubal TV, Dharmadhikari S, Abdulla AM, Arora S, Rawal S, & Kesharwani P (2022) Review on synthesis, properties and multifarious therapeutic applications of nanostructured zirconia in dentistry *RSC Advances* **12**(20) 12773-12793. <https://doi.org/10.1039/d2ra00006g>
 23. Blatz MB, Sadan A, & Kern M (2003) Resin-ceramic bonding: A review of the literature *Journal of Prosthetic Dentistry* **89**(3) 268-274. <https://doi.org/10.1067/mpr.2003.50>
 24. Kim H-K, Yoo K-W, Kim S-J, & Jung C-H (2021) Phase transformations and subsurface changes in three dental zirconia grades after sandblasting with various Al₂O₃ particle sizes *Materials (Basel)* **14**(18) 5321. <https://doi.org/10.3390/ma14185321>
 25. McLaren EA, Lawson N, Choi J, Kang J, & Trujillo (2017) New high-translucent cubic-phase-containing zirconia: Clinical and laboratory considerations and the effect of air abrasion on strength *Compendium of Continuing Education in Dentistry* **38**(6) e13-e16. <https://pubmed.ncbi.nlm.nih.gov/28586235/>
 26. Wille S, Zumstrull P, Kaidas V, Jessen LK, & Kern M (2018) Low temperature degradation of single layers of multilayered zirconia in comparison to conventional unshaded zirconia: Phase transformation and flexural strength *Journal of the Mechanical Behavior of Biomedical Materials* **77** 171-175. <https://doi.org/10.1016/j.jmbbm.2017.09.010>
 27. Nagaoka N, Yoshihara K, Tamada Y, Yoshida Y, & Van Meerbeek B (2019) Ultrastructure and bonding properties of tribochemical silica-coated zirconia *Dental Materials Journal* **38**(1) 107-113. <https://doi.org/10.4012/dmj.2017-397>
 28. Matinlinna JP, Lung CYK, & Tsoi JKH (2018) Silane adhesion mechanism in dental applications and surface treatments: A review *Dental Materials* **34**(1) 13-28. <https://doi.org/10.1016/j.dental.2017.09.002>
 29. Porojan L, Vasiliu R-D, Birdeanu M-I, & Porojan S-D (2020) Surface characterization and optical properties of reinforced dental glass-ceramics related to artificial aging *Molecules* **25**(15) 3407. <https://doi.org/10.3390/molecules25153407>
 30. Lung CYK, Liu D, & Matinlinna JP (2015) Silica coating of zirconia by silicon nitride hydrolysis on adhesion promotion of resin to zirconia *Materials Science and Engineering. C, Materials for Biological Applications* **46** 103-110. <https://doi.org/10.1016/j.msec.2014.10.029>

